

GAMMA-RAY BURST PROGENITORS CONFRONT OBSERVATIONS

DAVIDE LAZZATI

*Institute of Astronomy, University of Cambridge
Madingley Road, CB3 0HA, Cambridge
United Kingdom*

The discovery of a supernova emerging at late times in the afterglow of GRB 030329 has apparently settled the issue on the nature of the progenitor of gamma-ray bursts. We now know that at least a fraction of cosmological GRBs are associated with the death of massive stars, and that the two explosions are most likely simultaneous. Even though the association was already suggested for GRB 980425, the peculiarity of that burst did not allow to extend the association to all GRBs. The issue is now to understand whether GRB 030329 is a “standard burst” or not. I will discuss some peculiarities of GRB 030329 and its afterglow lightcurve showing how, rather than a classical cosmological GRB, it looks more like a transition object linking weak events like GRB 980425 to the classical long duration GRBs. I will also discuss the problems faced by the Hypernova scenario to account for the X-ray features detected in several GRBs and their afterglows.

1. Introduction

The progenitor of Gamma-Ray Bursts (GRBs) - i.e. the astronomical object that is associated to the energy release powering the GRB emission, and that probably disappears in the process - has been a major unknown since their discovery in the late sixties¹. Since the discovery of afterglow emission^{2,3}, that made possible their precise localisation in the sky, several circumstantial pieces of evidence have been collected, linking the burst emission with massive star formation phenomena^{4,5,6,7,8}. Even though such studies pointed toward an association of GRB explosions with the death of massive stars, the issue was far from being solved, the main worry being that multi-wavelength modelling of afterglows yielded typically a uniform ambient medium⁹, contrary to the stratified wind expectations for the massive star association¹⁰.

The exact association of the burst with the star death was therefore put under debate. The simplest scenario (Hypernova or Collapsar) would call for a single explosion, in which the GRB would be produced by a relativistic jet propagating along the rotational axis of a fast spinning star, which explodes as a more normal supernova along the equator¹¹. Alternatively, the two explosions (SN and GRB) could be separated by a relatively short interval of time (Supranova), during which a metastable compact object is left, whose eventual collapse cause the GRB explosion¹². Finally, new population synthesis studies showed that neutron star binary systems

may be short lived, allowing for the GRB explosion within the host galaxy¹³ even in the classical binary merger scenario¹⁴.

The association of the peculiar GRB 980425 with SN1998bw¹⁵ and, more recently, that of GRB 030329 with SN2003dh^{16,17} and of GRB021211 with SN2002lt¹⁸ has given strong support to the idea of a single explosion, which simultaneously generates a GRB and a particularly energetic SN explosion. There is however a number of observations that seem to point to a more complex association. The issue is therefore to understand whether GRB 980425 and GRB 030329 are “classical GRBs” and to which extent all the observations can be incorporated in a single coherent picture.

In this review I will critically discuss some aspects of this problem, underlying possible peculiarities of the prompt and afterglow emission of the two bursts robustly associated to SN explosions. I will then discuss progenitor indications from X-ray spectroscopy of the prompt and afterglow emission, discussing the problems that arise when we attempt to include these observations in a simple Hypernova scenario

2. Collapsars & Hypernovæ

The observation of non-thermal high energy power-law tails in GRB spectra, well above the pair production threshold $h\nu = m_e c^2 = 511$ keV allows us to draw to fundamental conclusions. First, the photon producing medium must be outflowing at hyper-relativistic speed, with $\Gamma \gtrsim 100$, to avoid the absorption of photons above threshold. Second, to preserve the non-thermal character of the spectrum, the moving plasma must contain a small but sizable amount of baryons, of the order of $M_0 \sim 10^{-4} M_\odot$. In other words, the baryon contamination of the fireball, even if non negligible, must be extremely small. This limit is particularly stringent for any model in which the relativistic GRB jet has to find its way through a massive star.

A wide relativistic jet (where wide means such that $\theta_j > \Gamma^{-1}$) that propagates through a medium collects all the material ahead of itself since, due to the relativistic aberration of trajectories, the stellar material cannot flow to the sides of the jet¹⁹. For this reason, a relativistic jet would be engulfed with the stellar material and effectively slowed down to sub-relativistic speed. Even if the jet is generated as a relativistic flow in the core of the star, it will drive a bow shock at its head, which will advance at sub-relativistic speed pushing the dense stellar matter on the sides. In this process part of the jet bulk energy is randomised and lost from the relativistic flow. It may be recycled in a second time, when the engine turns off, in the form of a delayed wide-angle fireball component²⁰.

Numerically, the jet evolution has been studied extensively under varied conditions, both to understand how it propagates into the star^{11,21} and the effect on the stellar explosion²². Figure 1 shows some of the more recent results by Zhang et al.²¹. In all these studies the jet is postulated at the core of the star while, more recently, MHD simulations for the jet formation have been performed²³.

A first constraint on the properties of the progenitor star is its radius. Being

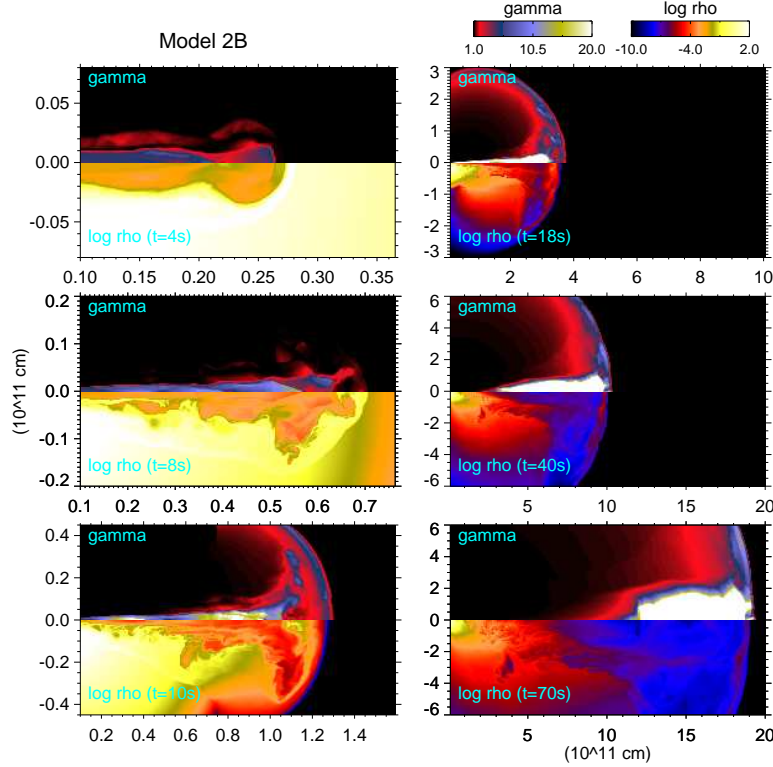


Figure 1. Results of relativistic simulations for the propagation of a jet in a compact stellar core. From Zhang et al.²¹.

non-relativistic, the jet spends a time^a $t \gtrsim R_*/c \sim 3 R_{\{\star,11\}}/c$ to propagate through the star mantle. During all this time, the inner engine has to be on, to sustain the propagation of the jet head. This time is lost, in the sense that the energy released is not seen in the GRB emission. In order to avoid a fine tuning in the distribution of the duration of long GRBs and to explain the “standard GRB energy”^{24,9}, we must conclude that the propagation time is much shorter than the burst duration, and therefore $R_* < 10^{11} \text{ cm}$ ¹¹. The star has therefore lost all the hydrogen and helium envelopes through a wind (Wolf Rayet phase) or the interaction with a close companion in a binary system²⁵. Since a massive wind would probably also cause the loss of angular momentum (another fundamental ingredient in the recipe for successful jet propagation), the latter possibility seems favoured.

In terms of populations, there are many more type Ibc SNe than GRB explosions, and therefore the loss of the envelope seem not to be the sufficient ingredient for a successful jet propagation, confirming the idea that an additional condition must be

^aHere and in the following we adopt the notation $Q = 10^x Q_x$ and use c.g.s. units.

fulfilled. Interestingly, to date, the only robust associations with GRBs are for type Ic SNe, these without trace of either hydrogen and helium in their spectra^{15,16,17}.

3. Supranovæ

Supranovæ were proposed as possible progenitors for GRB explosions in order to solve the problem of baryon contamination without losing the association of GRBs with the death of a massive star. The main characteristic feature of a supranova explosion is that is made by two explosions. At the end of its life, a massive star explodes as a SN, leaving behind a compact unstable object. This, in the most popular version of the model, is a massive neutron star (NS), too massive to be stable and avoid the implosion into a black hole. Most NS equations of state, however, allow for meta-stable super-massive objects if the NS is fastly spinning, so that the centrifugal support provides the extra pressure is required to keep the configuration stable¹². If the newly born NS has a sizable magnetic field which is not perfectly aligned with its rotation axis, the NS will lose energy as a pulsar, at the expenses of rotational energy. As the NS slows down its rotation, the condition for stability is lost and the system collapse into a black hole. This collapse is supposed to power the GRB.

Vietri and Stella¹² computed the lifetime of the system to be:

$$t_{\text{sd}} \equiv \frac{J}{\dot{J}} = 10 \frac{j}{0.6} \left(\frac{M}{3 M_{\odot}} \right)^2 \left(\frac{15 \text{ km}}{R_{\text{NS}}} \right)^6 \left(\frac{10^4 \text{ s}^{-1}}{\omega} \right)^4 \left(\frac{10^{12} \text{ G}}{B} \right)^2 \text{ yr} \quad (1)$$

and therefore the GRB explosion site should, in this model, be surrounded by a relatively young SNR of radius:

$$R_{\text{SNR}} \sim 3 \times 10^{17} \frac{j}{0.6} \left(\frac{M}{3 M_{\odot}} \right)^2 \left(\frac{15 \text{ km}}{R_{\text{NS}}} \right)^6 \left(\frac{10^4 \text{ s}^{-1}}{\omega} \right)^4 \left(\frac{10^{12} \text{ G}}{B} \right)^2 \left(\frac{v_{\text{SNR}}}{10^4 \text{ km/s}} \right) \text{ cm} \quad (2)$$

the result is strongly dependent on initial conditions, and therefore the model predicts a range of time delays (and consequent SNR radii). The presence of the nearby SNR, as we shall see in the following, is particularly important to explain some of the observed X-ray features. The explosion of the GRB inside a magnetised cavity may as well ameliorate the problem of magnetic field generation and explain the uniform ambient media derived from afterglow modelling²⁶.

4. Prompt emission

The association of GRB 030329 with the supernova SN2003dh bears much more important consequences than that of GRB 980425 with SN1998bw. While GRB 980425 is a peculiar GRB, with an energy budget which is largely smaller than that of classical GRBs, GRB 030329 is, at face value, a typical cosmological burst. In this section and in the following I discuss the properties of GRB 030329 and compare them to those of high redshift GRBs.

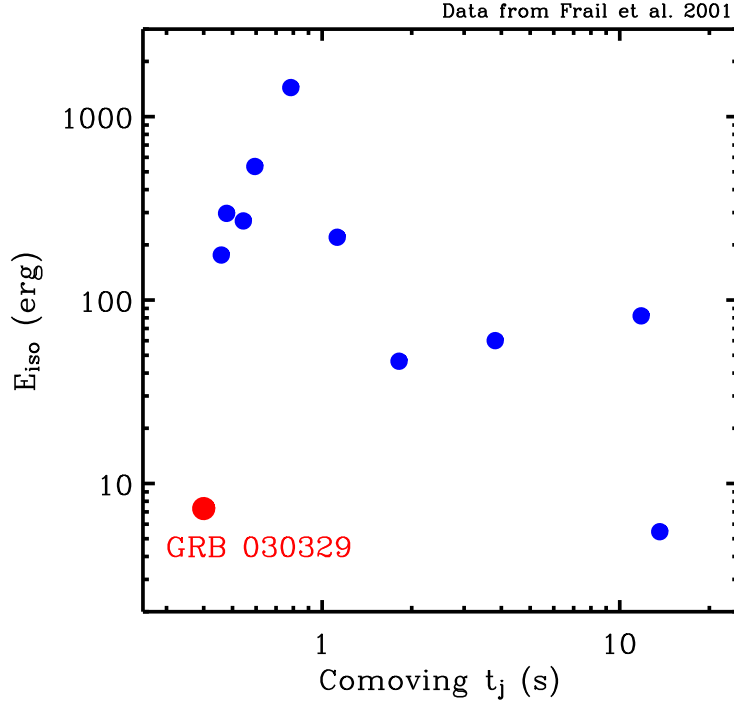


Figure 2. Isotropic equivalent energy release in γ -rays vs. jet break time for a sample of “classical” GRBs and GRB 030329, which is under-energetic in this plane.

4.1. Standard Energy

One of the most important results in GRB studies of the last few years is the realisation that the total energy budget of the event, once corrected for the opening angle of the jet^b is fairly typical, amounting to $E \sim 10^{51}$ erg^{24,9}.

This value is certainly not attained by GRB 980425 which, even for a spherical explosion, had a total energy release in ultra-relativistic material $E \lesssim 10^{48}$ erg. The case of GRB 030329 is more complicated. The isotropic energy release of GRB 030329 is fairly typical for a dim burst, but the afterglow light curve has a clear break at early times $t_b \sim 0.4$ d, which allows us to infer a small opening angle. In Fig. 2 I show the correlation between the isotropic equivalent energy and the break time for several classical GRBs (which form a clear correlation) and GRB 030329. It is clear that, given the break time, the energy is smaller by more than an order of magnitude with respect to what predicted by the correlation.

Given the complexity of the afterglow light curve of GRB 030329 (see below) it

^bIn the framework of the universal structured jet the correction is performed on the viewing angle rather than on the opening angle of the jet²⁷.

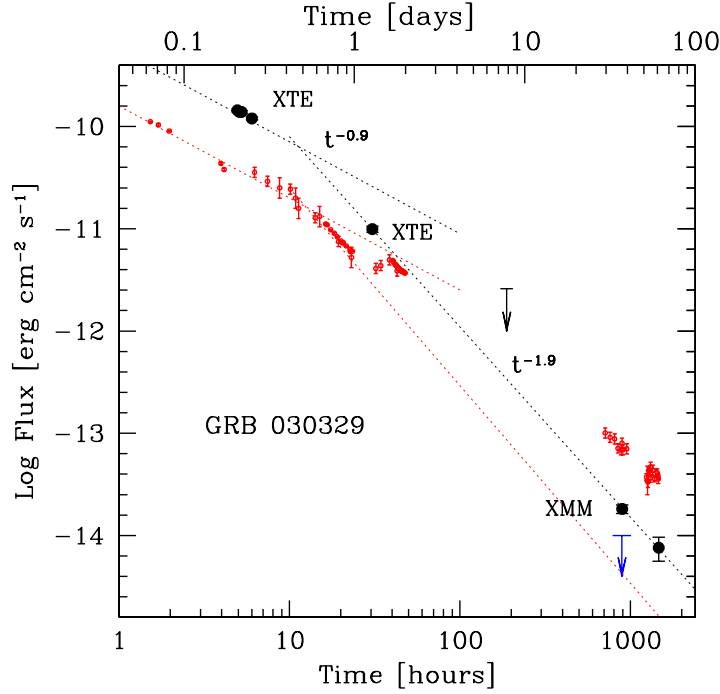


Figure 3. Optical and X-ray light curves of GRB 030329, showing that the break in the optical is simultaneous with the break in the X-rays, as predicted for a jet transition. From Tiengo et al.²⁸.

is however worth asking ourselves whether the break is really a jet break and not a spectral transition or merely a fluctuation on top of a regular power-law decay. Fortunately several X-ray observations, both from the Rossi-XTE and XMM, are available to confirm that the break is achromatic²⁸, as predicted for a jet break. The break in GRB 030329 is actually the best example of an achromatic break in an afterglow we have to date (see Fig. 3).

4.2. Typical photon energy

Another interesting correlation that was discovered in classical long GRBs is the correlation between the isotropic equivalent energy and the peak of the $\nu F(\nu)$ spectrum^{29,30}. The correlation is shown in Fig. 4, where GRB 030329 and GRB 980425 are indicated individually. While GRB 030329 fits the correlation, fostering its appartaining to the classical GRB family, GRB 980428 stands out, underlying again its peculiarity.

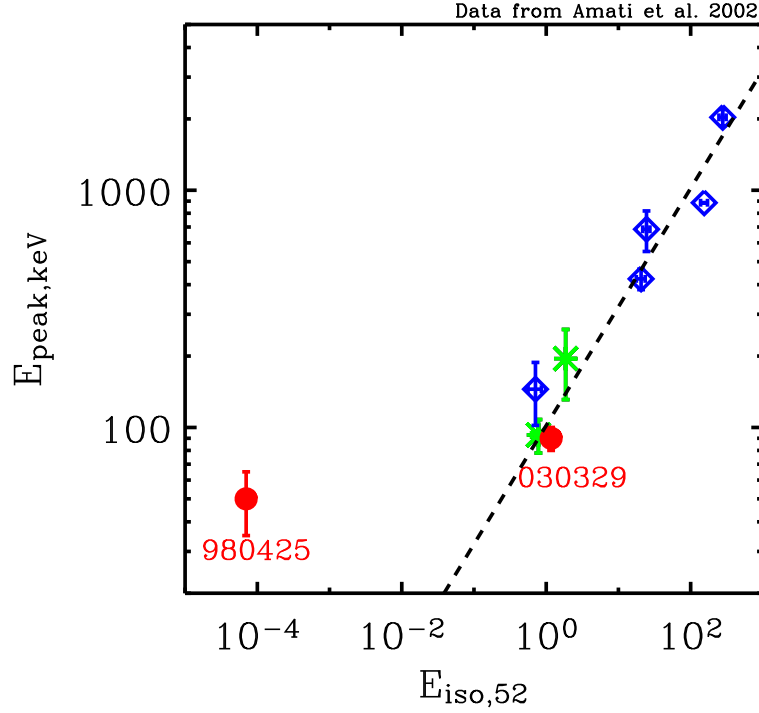


Figure 4. Isotropic equivalent energy versus peak photon frequency (in $\nu F(\nu)$ representation). Diamonds show high redshift events, for which no SN association is claimed, asterisks show intermediate redshift events, for which the SN association is based on red bumps in the late afterglow evolution. GRB 030329 and GRB 980428 are shown with dots and indicated.

5. Afterglow

The phase in which GRB 030329 shows more peculiarities is the afterglow. Whether this is due to an intrinsic difference with respect to other GRBs or rather to a difference in the conditions of the ambient medium is not clear and worth a deeper investigation.

5.1. Bumps and wiggles

The multi-filter afterglow light curve of GRB 030329 is shown in Fig. 5. A first important thing to understand is whether the complexity of the afterglow light curve is intrinsically larger than in other GRBs or simply more apparent given the enormous observational effort devoted to this particular afterglow³¹. In comparison one can think to the case of GRB 020813, the smoothest afterglow studied so far^{32,33}, for which 55 photometric V-band observations were collected.

To test the possibility that the light curve of GRB 020813 appears smooth only due to a lack of coverage we have simulated 10000 fake R-band light curves by randomly selecting 55 photometric measurements from the ~ 1600 from the light curve

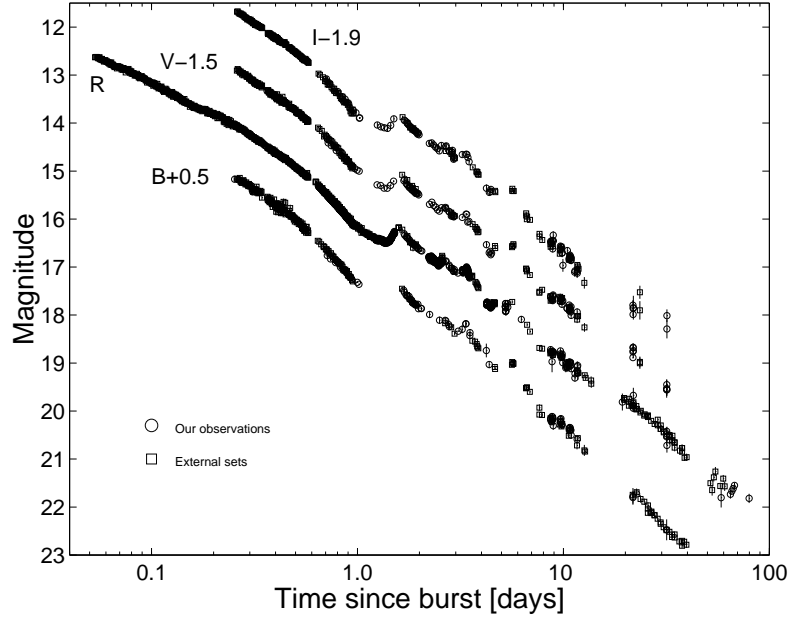


Figure 5. Optical BVRI light curve of GRB 030329. The amount of photometric measurements performed on this event is unprecedented and the light curve reveals a complex behaviour on top of the usual broken power-law decay. From Lipkin et al.³¹.

of GRB 030329 (data table taken from Lipkin et al.³¹). For each simulated light curve we have attempted to fit a smoothly broken power-law shape and estimated the goodness of fit with the reduced χ^2 . The procedure was repeated twice. First we assigned the real error bars to the data. Subsequently the photometric accuracy was reduced by assigning a minimum uncertainty of 0.05 magnitudes to each point. The distribution of the resulting reduced χ^2 values is reported in Fig. 6. For no single case out of 20000 total simulations an acceptable χ^2 was obtained, not even with the reduced accuracy of the photometry. We are therefore able to conclude that the afterglow of GRB 030329 represents a case of intrinsically high variability, much larger than what observed in most cosmological afterglows. To further deepen this analysis we reduced the number of photometric observations. We find that only if the number of photometric points is reduced to less than 10 the simulated light curves can be effectively described as broken power-laws: $\sim 2\%$ of the light curves with 10 photometric points and $\sim 11\%$ of these with 5 yield $\chi^2_{\nu} \leq 2$.

An interesting issue is the origin of the observed afterglow complexity. One important observation that helps reducing the possibilities is the fast rise-time of the bumps. Any event (increase or decrease of brightness) that takes place over the entire fireball surface will be observed to smoothly affect the afterglow light curve over a timescale $\delta t \sim T$, where T is the moment in which the deviation begins³⁴. Since the increase in brightness in GRB 030329 is much faster it must be due to a

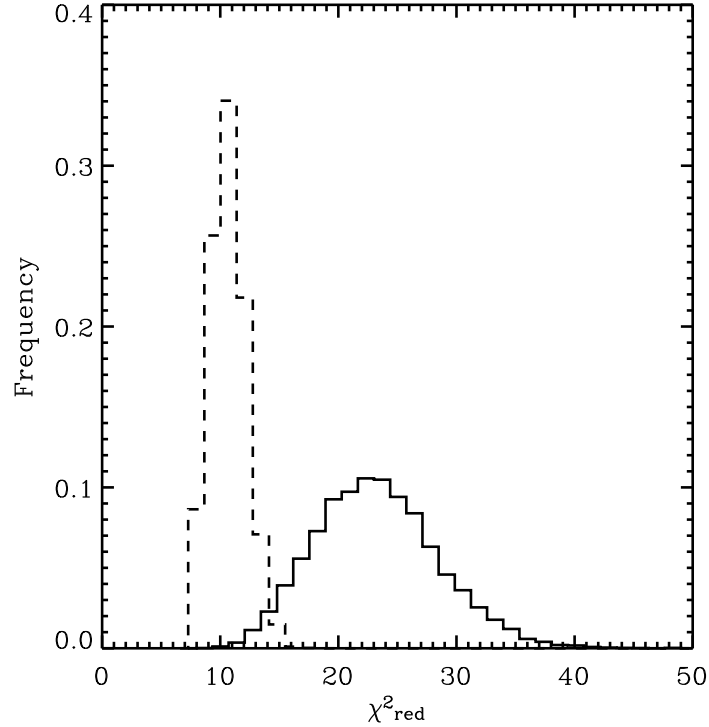


Figure 6. Distribution of χ^2 values for two set of 10000 simulations each of reduced quality light curves drawn from real R-band observations of GRB 030329 (see text for more details). The solid histogram refers to simulations with 55 observational points without reducing the accuracy of the measurement, while the dashed histogram is for simulations where a minimum uncertainty of 0.05 magnitudes was assumed for the photometry.

local phenomenon. Another clue comes from the fact that the fireball is observed to monotonically brightens instead of showing random increases and decreases in brightness. For these reasons the best solution seems to be a late time input of energy from the inner engine³⁵, under the form of delayed shells. Since the extra energy is input in the fireball after the jet break time, it does not involve the entire fireball surface and can be characterised by a rise time $\delta t < T$. A very important implication of this model is that, given the prominence of the rebrightenings, the extra energy input is larger by an order of magnitude than the original ejected energy. If this extra energy is considered in Fig. 2, the GRB 030329 point would move upward by more than a factor of ten, making GRB 030329 consistent with the correlation.

The only problem for this interpretation is the polarization curve³⁶. If the extra energy input is always given to the same part of the fireball, the polarization curve should show a marked correlation between the rebrightenings and the polarization

intensity and position angle, something that is not observed in the data. However, it is possible to argue that the refreshed shock will not be completely uniform, giving rise to unpredictable fluctuations in the polarization signal.

5.2. *Structure?*

An alternative interpretation for the complexity of the GRB 030329 afterglow light curve can be formulated based on the peculiarity of its radio light curve. It shows a prominent break at $t \sim 10$ d³⁷, which has all the properties of a second jet break. Berger et al.³⁷ interpret it as due to a second component in the fireball, with lower energy per unit solid angle and Lorentz factor, but larger opening angle and larger total energy by a factor 10. It turns out that a refined analysis of the optical lightcurve requires as well a second break at $t \sim 10$ d, as expected for a jet break. The two components of the fireball may have been simultaneous, in a structured jet scenario²⁷ or delayed in time as well, the slower one being produced by the recycling of the energy the jet wasted in the process of opening up a clean funnel in the star²⁰. Even though this interpretation explains the overall shape of the light curve, it faces several problems to explain the rapidity of fluctuations and the fact that not a single rebrightening is observed. The extra ingredient of delayed energy input is therefore still necessary. Also in this case, however, the standard GRB energy of $\sim 10^{51}$ erg would be recovered.

6. X-ray features

The most serious challenge to extending the hypernova origin of GRB 030329 to all cosmological GRBs is represented by the possible presence of X-ray narrow features, both in absorption and emission, in the prompt and early afterglow emission of several bursts^{38,39,40,41,42,43}. The best examples of absorption and emission line are shown in Figures 7, 8 and 9.

Even though the reality of the features has been challenged on the statistical ground, it should not be forgotten that they have been detected with five different instruments consistently (even though no single feature has been detected independently in more than one detector). There are now seven detected narrow features (or system of features) in emission in the early afterglow⁴⁴ and 2 transient absorption features during the early prompt emission⁴³.

6.1. *Emission features*

The detection of bright narrow emission features in the early X-ray afterglow requires the presence of dense reprocessing material in the surrounding of the burster⁴⁵. The features are detected at the rest frame frequency of the host galaxy, and cannot therefore be produced within the fireball, which is still, at that time, approaching the observer with $\Gamma > 10$.

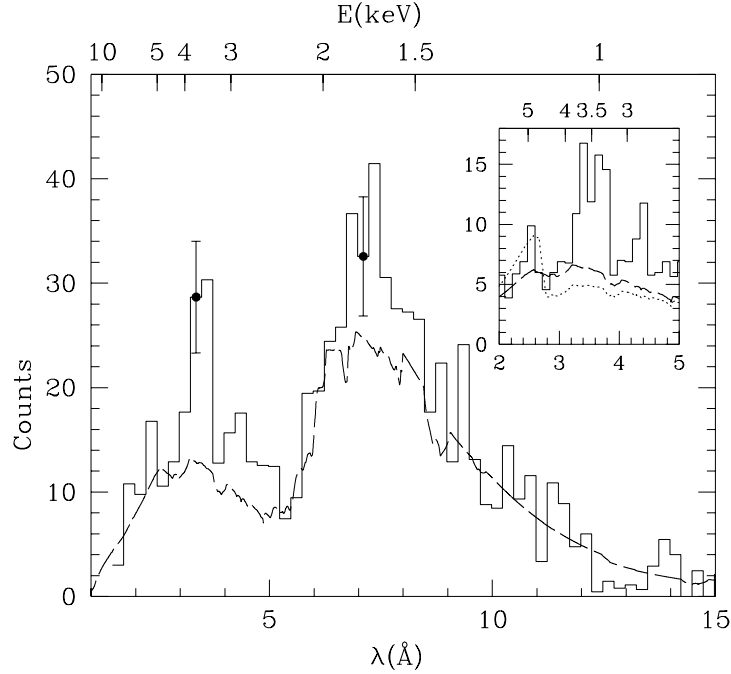


Figure 7. The Chandra grating spectrum of the early X-ray afterglow of GRB 991216 showing evidence of a broadened X-ray emission line. From Piro et al.⁴⁰.

Let us consider as an example case iron lines. The typical line luminosity is $L_{\text{Fe}} \sim 10^{44}$ erg s⁻¹ and the lines are detected for a time $t_{\text{Fe}} \gtrsim 10^5$ s. This allows us to compute the total number of photons in the line as:

$$N_{\text{Fe}} = \frac{L_{\text{Fe}} t_{\text{Fe}}}{\epsilon_{\text{Fe}}} \sim 10^{57} \quad (3)$$

which yields a total mass of the reprocessing material of:

$$M_{\text{tot}} \sim \frac{m_p N_{\text{Fe}}}{A_{\text{Fe}} k} = \frac{2 \times 10^4}{A_{\text{Fe},\odot} k} M_{\odot} \quad (4)$$

where A_{Fe} is the iron abundance in number, $A_{\text{Fe},\odot}$ is the iron abundance in solar units and k is the number of line photons that each iron ion emits. It is clear that, even allowing for a highly iron enriched material, we need $k \gg 10$. An isolated iron ion, taking into account the Auger yield, can emit up to 12 line photons. The only way to increase the value of k is by allowing for recombination of free electrons on the iron ion on a timescale comparable to the burst and early afterglow duration. Since the recombination timescale is inversely proportional to the free electron density,

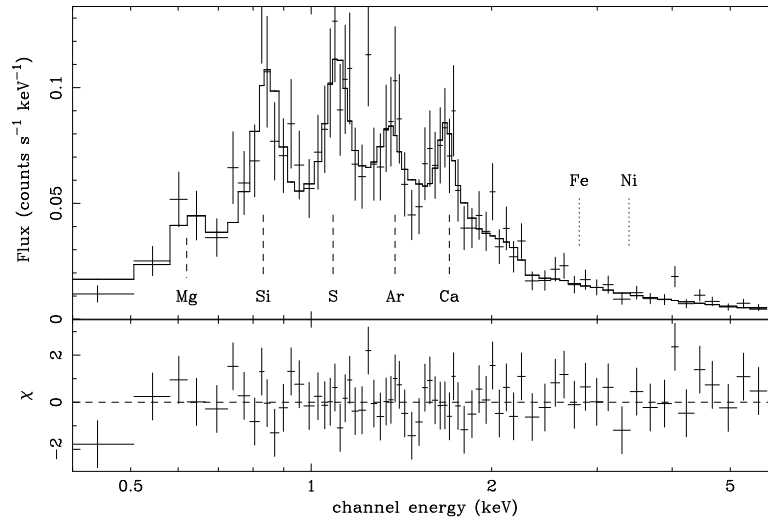


Figure 8. The XMM-Newton spectrum of the early X-ray afterglow of GRB 030227 showing evidence of a complex of soft X-ray emission lines. From Watson et al.⁴².

we obtain that the density of the reprocessing material must satisfy:

$$n \gtrsim 10^{10} \text{ cm}^{-3} \quad (5)$$

Such a high density poses new problems. It cannot be ahead of the fireball, since it would slow down the fireball to sub-relativistic speed in a short time interval, contrary to observations. Two solutions have been proposed. In the class of Geometry Dominated (GD) models^{45,46,47,48,49}, the reprocessing material is supposed to be concentrated in an asymmetric toroidal or funnel-like structure around the GRB explosion site. The most natural progenitor that could provide such a geometry is the SN remnant of a Supranova. In the class of Engine Dominated (ED) models^{50,51}, the reprocessing material is provided by the exploding star itself (in the framework of collapsars) and lies behind the fireball. For this reason the ionising continuum cannot be provided by burst and/or afterglow photons and a delayed energy release from the inner engine has to be postulated.

The properties of the two models are discussed elsewhere in these proceedings⁴⁴ and we therefore discuss here only the problems facing the ED scenario, given the focus of this contribution in discussing whether a hypernova origin can be confirmed for all classical long-duration GRBs.

The first question ED models face is why we see iron lines. Even though iron lines are the most common features in X-ray spectroscopy, if the reprocessing material is provided by the exploding star, it should be rich in nickel rather than in iron⁴⁷. This is due to the fact that in SN explosions ⁵⁶Ni is synthesised, which decays in ⁵⁶Co and eventually, after a timescale of ~ 100 days, into the stable isotope of ⁵⁶Fe. In a simultaneous explosion scenario the reprocessing material should therefore be

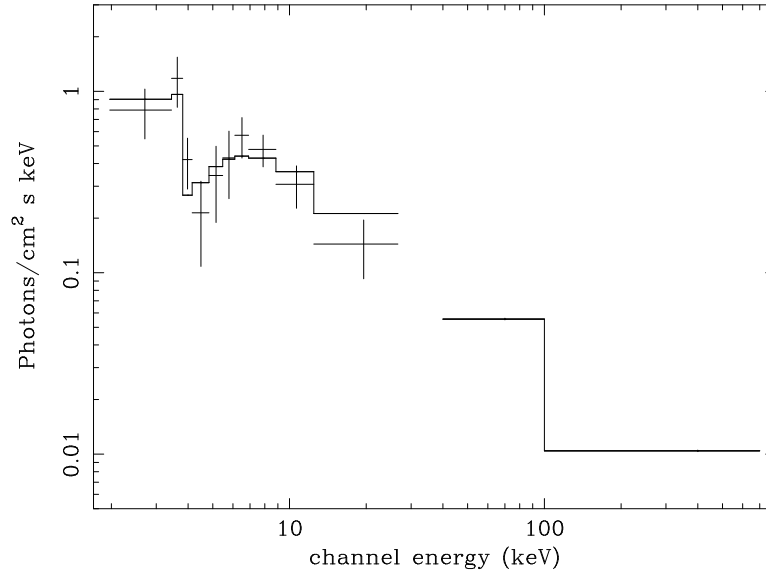


Figure 9. The BeppoSAX-WFC and GRBM combined spectrum of the early X-ray prompt emission of GRB 990705 showing evidence of a deep absorption feature. From Amati et al.⁴³.

nickel rich. There are two possible solutions to this problem. The first is that there are areas in the SN explosion parameter space where ^{54}Fe is synthesised directly. Such supernovae, however, should have a particularly dim light curve, lacking the energy input from the decay of the unstable Ni and Co isotopes. This contradicts the presence of SN bumps in many afterglow^c. Alternatively, it has been argued that the line may be intrinsically from Ni, but downscattered to the Fe energy on the walls of the funnel through which the GRB propagates⁵². This solution, besides requiring somewhat fine tuned parameters, faces the problem of efficiency. Each scattering reduces by a factor of ~ 2 the number of photons, with the result that the energy that goes into the line production is at least 100 times larger than the available energy in the GRB explosion⁵³.

The second problem is why in some afterglow we see iron lines and in some others we see only lighter elements (Si, S, Ar and Ca). In the case of GD models, this can be due to a different ionisation parameter for the reprocessing material⁴⁸, as a function of the different time delay between the SN and the GRB explosion. Short delays would produce soft X-ray lines, the Fe group ones being quenched by the Auger effect, while longer delays would produce Fe lines. In the ED model, there seems to be much less space for changing parameters in a natural way.

A final problem is represented by the large equivalent width (EW) of the soft

^cIt should be clarified here, however, that in no case to date a simultaneous detection of a SN bump and of X-ray features has been possible

X-ray lines in GRB 011211⁴¹. In any reflection model (optically thin line production is not efficient enough) the EW of the lines depends on which fraction of the illuminating continuum can reach the observer. If all the continuum reaches the observer, the EW of soft X-ray lines has to be small, ~ 150 eV at most. The only way to explain the ~ 500 eV EW detected in 011211⁴¹ is by allowing for a pure reflection spectrum, where the ionising continuum is completely hidden to the observer. In a simultaneous explosion only a very contrived geometry can provide such a condition, which is naturally fulfilled in GD models since the line emission reaches the observer when the continuum has already faded by several orders of magnitude⁴⁸.

6.2. Absorption features

The hardest challenge to simultaneous explosion models is however the presence of transient absorption features in the spectra of at least one, possibly two, GRBs. These features are detected in the early phases of the GRB X-ray prompt emission and disappear after tens of seconds. The best case we have so far is that of GRB 990705⁴³ in which a deep absorption feature was detected during the first 13 seconds of the prompt emission. The feature, if identified as an Fe absorption edge, allows a redshift measurement that was subsequently confirmed by optical spectroscopy of the host galaxy, dramatically confirming the reality of the feature. The feature was initially interpreted as an absorption edge from neutral iron⁴³. Such an interpretation requires however an extremely large amount of iron at sub-parsec distances from the burster and was subsequently abandoned in favour of a broadened resonant feature from highly ionised iron and cobalt⁵⁴.

The transient nature of the feature is of great importance, since it allows us to measure the distance of the absorber from the GRB source⁵⁵. The derived distance depends slightly on the assumed origin of the feature (either edge or resonant line). We make here the example of the resonant scattering line, which requires a less dramatic amount of iron group absorbing nuclei. In this case the absorbing material must be dense enough to allow for a recombination timescale $t \lesssim 10$ s and the quenching of the absorption is due not to the complete ionisation of the iron ions but to the heating of the absorbing medium by Inverse Compton (IC) interactions of the free electrons with the GRB photons. The IC heating time scale is given by⁵⁴:

$$t_{\text{IC}} \sim \frac{4\pi R^2 \epsilon}{L \sigma_T} \quad (6)$$

where R is the distance of the absorber from the burst explosion site, ϵ is the typical photon energy and L the burst luminosity in the keV band. Inserting the relevant numbers for GRB 990705⁴³ one obtains⁵⁴:

$$R \sim 2.6 \times 10^{16} \quad \text{cm} \quad (7)$$

and, to fulfil the requirement on the recombination time

$$n_e \sim 10^{11} \text{ cm}^{-3} \quad (8)$$

Such conditions cannot be satisfied by any stellar wind, however dense, while they are natural in a moderately clumped young supernova remnant.

7. Discussion

In this paper I have tried to address two questions: is GRB 030329 a typical GRB so that we can safely claim that all GRBs are associated to SNe and that the time delay between the two explosions is negligible? And the second: is there any evidence that is inconsistent with the above conclusion from independent observations?

The answer to the first question is that indeed GRB 030329 is much more similar to a classical cosmological GRB than GRB 980425, the first to be associated to the explosion of a massive star. The similarity of GRB 030329 with “classical GRBs” is however not complete. First there is evidence that the energy released by GRB 030329 in gamma-rays is smaller than usual by an order of magnitude, even though taking into account the energy released by the inner engine in the form of less relativistic material brings back the total energy budget to the “standard” $E = 10^{51}$ erg observed in cosmological GRB explosions^{24,9}. Secondly, and possibly related to the delayed energy input of energy, the afterglow lightcurve is much more complex than any previously observed GRB, and we showed that this is not due to the more complete sampling, but to an intrinsic variability that is unprecedented in cosmological GRBs.

An intriguing possibility is that there is a standard inner engine, possibly a black hole surrounded by a dense hot accretion disk, which releases a fairly standard energy in the form of a relativistic jet. The jet has however to open its way into the star and this creates the diversity in the observed properties of GRBs. Different relevant properties of the star may be related to its pre-explosion radius and/or rotation. A compact fast spinning star should offer less resistance to the jet propagation along its polar axis, giving origin to a cosmological GRB, in which most of the jet energy can escape untouched and produce γ -ray radiation. A more extended or less rotating star may offer more resistance. In this case a sizable fraction of the jet energy should be used to open up a funnel in the star, so that the resulting GRB would look under-energetic. Part, if not all, this energy may be recycled in a delayed slower fireball component that would catch up with the relativistic jet and re-energise it at later times.

This unification picture shall however be taken with care, at least until a final word is said about the reality of X-ray absorption and emission features. These cannot be easily incorporated in a single SN/GRB explosion scenario. Even though none of the claimed features is incontrovertible in terms of statistical significance, they form a consistent set of observations all naturally predicted in the two explosion Supernova scenario¹². Instead of having a variable stellar radius and/or rotation, a

unification picture may call for a variable delay between the two explosions. Some delays are very short, and produce under-energetic GRBs, since part of the jet energy is wasted to reach the star surface. Short ($<$ several weeks) delays do not produce detectable γ -rays, since the jet is completely choked inside the optically thick SN remnant⁵⁶. Longer delays would instead produce a “classical GRB”, since the jet has no baryonic material to cross.

Also this simple scenario faces however some problems, since there are many “classical GRBs” that show sign of red bumps at late times, usually identified as the emergence of the SN lightcurve on top of the power-law afterglow decay^{57,58,59,60,61}. These SN explosion should be simultaneous to the GRB explosion. A unification scenario that would take into account all the observations with their most probable interpretations would therefore need to take into account the possibility of both a variability in the progenitor star properties and of the explosion delay.

I wish to thank S. Covino, F. Frontera, A. Königl, G. Ghisellini, P. Mazzali, R. Perna, E. Pian, M. J. Rees, E. Rossi, L. Stella and M. Vietri for the fruitful collaboration and discussions that led to the development of many of the ideas presented in this paper.

References

1. R. W. Klebesadel, I. B. Strong and R. A. Olson, *ApJ*, **182**, L85 (1973)
2. E. Costa et al., *Nature*, **387**, 783 (1997)
3. J. van Paradijs et al., *Nature*, **386**, 686 (1997)
4. S. R. Kulkarni et al., *Nature*, **393**, 35 (1998)
5. A. S. Fruchter et al., *ApJ*, **519**, L13 (1999)
6. S. Holland and J. Hjorth, *A&A*, **344**, L67 (1999)
7. J. S. Bloom, S. R. Kulkarni and S. G. Djorgovski, *AJ*, **123**, 1111 (2002)
8. D. Lazzati and R. Perna, *MNRAS*, **330**, 383 (2002)
9. A. Panaitescu and P. Kumar P., *ApJ*, **571**, 779 (2002)
10. R. A. Chevalier and Z. Li, *ApJ*, **520**, L29 (1999)
11. A. I. MacFadyen and S. E. Woosley, *ApJ*, **524**, 262 (1999)
12. M. Vietri and L. Stella, *ApJ*, **507**, L45 (1998)
13. R. Perna and K. Belczynski, *ApJ*, **570**, 252 (2002)
14. D. Eichler, M. Livio, T. Piran and D. N. Schramm, *Nature*, **340**, 126 (1989)
15. T. J. Galama et al., *Nature*, **395**, 670 (1998)
16. K. Z. Stanek et al., *ApJ*, **591**, L17 (2003)
17. J. Hjorth et al, *Nature*, **423**, 847 (2003)
18. M. Della Valle et al., *A&A*, **406**, L33 (2003)
19. C. D. Matzner, *MNRAS*, **345**, 575 (2003)
20. E. Ramirez-Ruiz, A. Celotti and M. J. Rees, *MNRAS*, **337**, 1349 (2002)
21. W. Zhang, S. E. Woosley and A. I. MacFadyen, *ApJ*, **586**, 356 (2003)
22. A. M. Khokhlov, P. A. Höflich, E. S. Oran, J. C. Wheeler, L. Wang and A. Y. Chtchelkanova, *ApJ*, **524**, L107 (1999)
23. D. Proga, A. I. MacFadyen, P. J. Armitage and M. C. Begelman, *ApJ*, **599**, L5 (2003)

24. D. A. Frail et al., *ApJ*, **562**, L55 (2001)
25. R. G. Izzard, E. Ramirez-Ruiz and C. A. Tout, *MNRAS in press*, astro-ph/0311463 (2004)
26. A. Königl and J. Granot, *ApJ*, **574**, 134 (2002)
27. E. Rossi, D. Lazzati and M. J. Rees, *MNRAS*, **332**, 945 (2002)
28. A. Tiengo, S. Mereghetti, G. Ghisellini, E. Rossi, G. Ghirlanda and N. Schartel, *A&A*, **409**, 983 (2003)
29. N. M. Lloyd, V. Petrosian and R. S. Mallozzi, *ApJ*, **534**, 227 (2000)
30. L. Amati et al., *A&A*, **390**, 81 (2002)
31. Y. M. Lipkin et al., *ApJ submitted*, astro-ph/0312594 (2004)
32. L. T. Laursen and K. Z. Stanek, *ApJ*, **597**, L107 (2003)
33. J. Gorosabel et al., *A&A submitted*, astro-ph/0309748 (2004)
34. D. Lazzati, E. Rossi, S. Covino, G. Ghisellini and D. Malesani, *A&A*, **396**, L5 (2002)
35. J. Granot, E. Nakar and T. Piran, *Nature*, **426**, 138 (2003)
36. J. Greiner et al., *Nature*, **426**, 157 (2003)
37. E. Berger et al., *Nature*, **426**, 154 (2003)
38. L. Piro et al., *ApJ*, **514**, L73 (1999)
39. A. Antonelli et al., *ApJ*, **545**, L39 (2000)
40. L. Piro et al., *Science*, **290**, 955 (2000)
41. J. N. Reeves et al., *Nature*, **416**, 512 (2002)
42. D. Watson, J. N. Reeves, J. Hjorth, P. Jakobsson and K. Pedersen, *ApJ*, **595**, L29 (2003)
43. L. Amati et al., *Science*, **290**, 953 (2000)
44. M. Böttcher, this volume (2004)
45. D. Lazzati, S. Campana and G. Ghisellini, *MNRAS*, **304**, L31 (1999)
46. M. Böttcher, *ApJ*, **539**, 102 (2000)
47. M. Vietri, G. Ghisellini, D. Lazzati, F. Fiore and L. Stella, *ApJ*, **550**, L43 (2001)
48. D. Lazzati, E. Ramirez-Ruiz and M. J. Rees, *ApJ*, **572**, L57 (2002)
49. F. Tavecchio, G. Ghisellini and D. Lazzati, *A&A in press*, astro-ph/0305265 (2004)
50. M. J. Rees and P. Meszaros, *ApJ*, **545**, L73 (2000)
51. P. Meszaros and M. J. Rees, *ApJ*, **556**, L37 (2001)
52. G. C. McLaughlin, R. A. M. J. Wijers, G. E. Brown and H. A. Bethe, *ApJ*, **567**, 454 (2002)
53. G. Ghisellini, D. Lazzati, E. M. Rossi and M. J. Rees, *A&A*, **389**, L33 (2002)
54. D. Lazzati, G. Ghisellini, L. Amati, F. Frontera, M. Vietri and L. Stella, *ApJ*, **556**, 471 (2001)
55. D. Lazzati, R. Perna and G. Ghisellini, *MNRAS*, **325**, L19 (2001)
56. D. Guetta and J. Granot, *MNRAS*, **340**, 115 (2003)
57. J. S. Bloom et al., *Nature*, **401**, 453 (1999)
58. D. E. Reichart, *ApJ*, **521**, L111 (1999)
59. T. J. Galama, *ApJ*, **536**, 185 (2000)
60. D. Lazzati et al., *A&A*, **378**, 996 (2001)
61. J. S. Bloom et al., *ApJ*, **572**, L45 (2002)